Max-Mahalanobis Anchors Guidance for Multi-View Clustering

Pei Zhang[1,2,3], **Yuangang Pan**[2,3], **Siwei Wang**[4], **Shengju Yu**[1], **Huiying Xu**[5*], **En Zhu**[1*]
Xinwang Liu[1*], **Ivor Tsang**[2,3]

[1] College of Computer Science and Technology, National University of Defense Technology, Changsha, 410073, China
[2] Centre for Frontier AI Research, Agency for Science, Technology and Research, 138632, Singapore
[3] Institute of High Performance Computing, Agency for Science, Technology and Research, 138632, Singapore
[4] Intelligent Game and Decision Lab, Beijing, 100091, China
[5] School of Computer Science and Technology, Zhejiang Normal University, Jinhua, 321004, China
{jeaninezpp, yuangang.pan, ivor.tsang}@gmail.com, {wangsiwei13, yu-shengju, enzhu, xinwangliu}@nudt.edu.cn

Abstract

Anchor selection or learning has become a critical component in large-scale multi-view clustering. Existing anchor-based methods, which either select-then-fix or initialize-then-optimize with orthogonality, yield promising performance. However, these methods still suffer from instability of initialization or insufficient depiction of data distribution. Moreover, the desired properties of anchors in multi-view clustering remain unspecified. To address these issues, this paper first formalizes the desired characteristics of anchors, namely *Diversity, Balance* and *Compactness*. We then devise and mathematically validate anchors that satisfy these properties by maximizing the Mahalanobis distance between anchors. Furthermore, we introduce a novel method called **M**ax-Mahalanobis **A**nchors **G**uidance for multi-v**I**ew **C**lustering (MAGIC), which guides the cross-view representations to progressively align with our well-defined anchors. This process yields highly discriminative and compact representations, significantly enhancing the performance of multi-view clustering. Experimental results show that our meticulously designed strategy significantly outperforms existing anchor-based methods in enhancing anchor efficacy, leading to substantial improvement in multi-view clustering performance.

1 Introduction

In the information era, various data forms provide distinct perspectives, but single perspective often overlooks the complexity and heterogeneity of data. For instance, in bioinformatics, behaviors of organisms are influenced by gene expression, protein-protein interaction and phenotypic characteristics. Isolating any single view may lead to incomplete conclusions (Rappoport and Shamir 2018). Multi-view clustering (MVC) tackles this by jointly analyzing multiple views to uncover their interrelations, with current methodologies focus on three core objectives: better representation (Gao et al. 2015; Sun et al. 2021; Yang et al. 2023), better alignment (Zhang et al. 2021; Wang et al. 2022) and better fusion (Kang et al. 2020a; Li et al. 2020; Zhang et al. 2023), which are also essential for handling missing views (Li et al. 2023b; Jin et al. 2023; Wen et al. 2023; Yu et al. 2024).

*Corresponding author.

The rapid growth of technology has led to a surge of multi-view data, providing new insights but posing challenges in large-scale data processing. Efficient clustering has emerged as a critical research focus, with mainstream approaches leveraging anchors to avoid associating all samples. This paper categorizes these anchor-based MVC methods into two groups: *fixed-anchor-based MVC* (Li et al. 2015; Li and He 2020; Kang et al. 2020b) and *optimized-anchor-based MVC* (Wang et al. 2021; Chen et al. 2022b; Li et al. 2023b; Ou et al. 2024). *Fixed-anchor-based MVC* typically generates anchors through pre-processing methods such as k-means or sampling strategies. Sampling methods, whether random or heuristic, are simple and efficient but often lead to poor and unstable performance due to randomness and weak structural relevance (Xia et al. 2022; Li et al. 2020). Besides, sampling may introduce more challenges, such as discrepancies in anchor correspondence across views. Instead, using k-means cluster centers as the anchors generally improves performance by leveraging clustering-relevant information in anchors (Kang et al. 2020b; Li and He 2020; Yang et al. 2022). However, k-means is sensitive to initialization, requiring multiple runs to mitigate randomness, and incorrect anchor initialization may cause disappointed clustering results. *Optimized-anchor-based MVC* improves upon the fixed-anchor strategy by incorporating anchors directly into the multi-view clustering optimization process. These methods typically employ the self-expression concept but use representative points to establish relationships with all samples. To ensure anchor representativeness, they generally impose orthogonal constraints to enforce diversity among anchors (Wang et al. 2021; Liu et al. 2022).

In summary, *fixed-anchor-based MVC* and *optimized-anchor-based MVC* each have distinct advantages and limitations. Fixed-anchor methods, derived from the original data space, aim to select anchors that better fit the data but face challenges with initialization instability and the complexity of heuristic design strategies. On the other hand, optimized-anchor methods learn anchors dynamically, making the acquisition of anchors less manual and more diverse through orthogonal constraints. However, these constraints can overly restrict anchor fitting performance, especially when the number of anchors is large.

Given the above research findings, this paper proposes an explicit definition of desirable anchors in multi-view clustering. In multi-view clustering, we expect to obtain a set of common anchors that possess three key properties: *Diversity*, *Balance*, and *Compactness*. Specifically, *Diversity* implies that the obtained anchors should be as dissimilar as possible, maximizing inter-cluster distances and facilitating more distinguishable data representations. *Balance* refers to the equilibrium between anchors across multi-view data, ensuring robust and stable structure. Data usually lie on a low-dimensional manifold within a high-dimensional space, exhibiting a more compact rather than uniform distribution. As a sketch of the data, the distribution of anchors should also maintain *Compactness* while satisfying the above two criteria, avoiding unnecessary increases in their dimensionality. Revisiting previous anchor-based methods with our defined anchor properties, we conclude that fixed-anchor methods mainly focus on balance, selecting anchors to effectively cover the data distribution. On the other hand, optimized-anchor methods emphasize diversity, striving to learn significantly different anchors to separate the data. However, orthogonal constraints on anchors may be overly restrictive, potentially limiting the model's representational capacity. Besides, this can impede data point discrimination in high-dimensional spaces due to the curse of dimensionality.

Since the ultimate goal of algorithmic models is to continuously fit data to anchors (either fixed or optimized), anchors with superior characteristics can guide the representation to be more discriminative, thereby achieving enhanced clustering performance. In light of the aforementioned analysis, we aim to provide an explicit definition of anchor properties and propose a design strategy for obtaining optimal anchors that satisfy these definitions. Integrating these anchors into our multi-view clustering framework can lead to superior data representations, thereby improving clustering performance. Specifically, we propose an optimal anchor design strategy called Max-Mahalanobis Anchors (MMA), which is carefully designed by maximizing the minimum angle between any two anchors, thereby achieving the promising iter-cluster dispersion effect. This paper then leverages the superior properties inherent in the MMA to achieve more efficacious re-representations of multi-view data, resulting in enhanced clustering performance. In summary, the main contributions of this paper are as follows:

- This paper provides formal definitions and mathematical formulation for the desirable properties (*Diversity, Balance* and *Compactness*) of anchors, revealing the deficiency of current anchor-based MVC methods.
- This paper proposes a rational-design anchor strategy, termed Max-Mahalanobis Anchors (MMA), satisfying the expected properties of anchors with theoretical proof. We integrate the novel MMA into our multi-view clustering framework, guiding the consensus representation to gradually align with our well-designed structure.
- Extensive experiments demonstrate our method's effectiveness. Comparisons with anchor-based MVC highlight our superior anchor performance and data fitting effects, validating the outstanding properties of MMA.

2 Related Work

In this section, we review the rationale and literature of anchor-based multi-view clustering methods. Then, the most relevant algorithms are introduced in detail. The key notations used throughout this paper are listed in Tab. 1.

Notation	Description
N, K, V	Number of samples, clusters and views
d_i	Feature dimension of i-th view
$\mathbf{X}^{(i)} \in \mathbb{R}^{N*d_i}$	Data matrix in the i-th view
$\mathbf{X}^{(i)}_{[j,:]}$	j-th row/sample in the i-th view
$\mathbf{e}_1$	The first unit basis vector
$\mathbf{0}_K$	The zero vector in $\mathbb{R}^K$
$\mathbf{I}_K$	Identity matrix of size K.

Table 1: Description of notations.

Anchor-based multi-view clustering methods have gained focus for their efficiency in large-scale scenarios, which involve using a small subset of representative points. Both fixed and optimized anchor-based methods fundamentally aim to associate original instances with a few representative points, thereby avoiding exploring global relationships.

Fixed-anchor methods in MVC typically determine anchors through random sampling, k-means or heuristic strategies for subsequent clustering tasks. While random sampling is simple and efficient, it often leads to unstable and unsatisfactory clustering results. Furthermore, researchers design meticulously crafted algorithms to directly sample data points as anchors (Xia et al. 2022). To enhance representativeness, Li et al. propose that anchors should comprehensively cover the data distribution, alternately sampling based on feature similarity across clusters. For more cluster-informed anchors, many studies rely on k-means clustering to generate fixed anchors (Li et al. 2015; Yang et al. 2020; Li and He 2020; Yang et al. 2022). Similarly, Kang et al. replace the self-expression in multi-view subspace clustering with anchor-samples expression, enabling subspace-based methods to scale to large clustering scenarios.

Unlike fixed-anchor approaches, optimized-anchor methods adopt an integrated framework to simultaneously optimize orthogonal anchors and construct anchor graphs. Representative studies (Sun et al. 2021; Wang et al. 2021) demonstrate that optimized-anchor are more representative than fixed ones and propose to optimize the orthogonal anchors and construct an anchor graph in a unified framework. Based on this, Liu et al. propose a one-pass approach to directly obtain the clustering labels by imposing graph connectivity constraints on the anchor graph (Liu et al. 2022). Subsequent variants of orthogonal optimization methods incorporate advancements in fusion (Zhang et al. 2023; Wang et al. 2022; Zhang et al. 2022; Li et al. 2023b), noise (Li et al. 2023a; Liu et al. 2024b), and graph constraints (Liu et al. 2024b,a; Yu et al. 2023; Li et al. 2024) and so on.

Despite the success of the current anchor-based MVC method over the earlier sampling methods, several essential issues persist. *Fixed-anchor-based* methods provide compu-

tational simplicity with improved fitness and balance in the original space. However, the inherent randomness of random sampling and k-means-based methods can undermine algorithmic stability. Moreover, designing anchor selection algorithms is often heuristic and challenging. *Optimized-anchor-based* methods enhance anchor diversity and reduce manual design effort through orthogonal constraints. Nevertheless, these constraints introduce a trade-off between fitting the data and maintaining orthogonality during optimization, limiting the compactness of representations. In summary, while existing anchor-based methods offer distinct advantages, the specific characteristics that anchors should possess for multi-view clustering have not yet been explicitly defined. To address this gap, the following sections formalize the definitions of anchor properties and introduce a novel method designed to satisfy them.

3 Methodology

This section begins with the definition of anchor properties and the construction of anchors. Then, we demonstrate its integration within our multi-view clustering framework.

3.1 Definition of Desired Anchors

In anchor-based multi-view clustering, we aim to obtain anchors with desirable properties to provide better guidance for multi-view data representation learning. Conceptually, we aspire for the anchors to exhibit properties of *Diversity, Balance,* and *Compactness*. However, it is challenging to constrain the anchors with these properties simultaneously. To achieve this, we propose to leverage the angular relationships between anchors and formulate the following three key definitions of anchor property.

Firstly, Definition 1 formalizes the concept of *Diversity* that the desired anchor should be as distinct as possible to facilitate discriminative capacity. We define this diversity metric by considering the mean of the angles between all unique pairs of anchors to be as large as possible, ensuring that anchors are apart from each other.

Definition 1 (**Diversity**). *Given a set of K anchors $\boldsymbol{\mu} = \{\mu_i\}_{i=1}^K$, the angle between any two distinct anchors μ_i and μ_j is defined as θ_{ij}. The average angle $\bar{\theta}$ is defined as $\bar{\theta} = \frac{2}{K(K-1)} \sum_{1 \le i < j \le K} \theta_{ij}$. If the condition $90^\circ \le \bar{\theta} \le 180^\circ$, or equivalently $-1 \le \cos\bar{\theta} \le 0$, is satisfied, the set of anchors $\boldsymbol{\mu}$ is characterized as possessing the Diversity property.*

Secondly, Definition 2 formalizes the concept of *Balance* that anchors should be distributed relatively uniformly, thereby creating a more robust and stable structure. We quantify balance by measuring the variance of angles between different anchor vectors.

Definition 2 (**Balance**). *Given $\boldsymbol{\mu} = \{\mu_i\}_{i=1}^K$, a set of K anchor. Angle θ_{ij} is defined for any two distinct anchors. If θ_{ij} satisfies the condition in Eq.* (1)*, the set of anchors $\boldsymbol{\mu}$ is characterized as possessing the Balance property.*

$$Var(\{\theta_{ij} | 1 \le i < j \le K\}) \le \varepsilon, \tag{1}$$

where $\theta_{ij} = \arccos\left((\mu_i^\top \mu_j)/(\|\mu_i\|_2 \|\mu_j\|_2)\right)$, ε is a non-negative threshold. $Var(\cdot)$ is the variance.

Last but not least, while satisfying *Diversity* and *Balance*, the anchor distribution should be as *compact* as possible, which means occupying as small space as possible and avoiding unnecessary increases in dimensionality.

Definition 3 (**Compactness**). *Given anchors $\boldsymbol{\mu} = \{\mu_i\}_{i=1}^K$, let $D = dim(\{\mu_i\}_{i=1}^K)$ denote the dimensionality of the space spanned by the anchors. Under the conditions specified by Definition 1 and Definition 2, if the D of one set of anchors is less than that of another set, then the set with the smaller D is said to possess better compactness.*

We have thus far presented three desirable properties of anchors. In the next subsection, we will introduce how to generate anchors that conform to these expectations.

3.2 Generate Max-Mahalanobis Anchors

Unlike previous approaches that relied on unstable initialization or rigid orthogonality constraints on anchors, we propose to simultaneously consider *Diversity, Balance, Compactness* criteria for anchors. Anchors satisfying these criteria leverage geometric properties for a diverse and uniform distribution of anchors within a compact space. Specifically, we propose a strategy called Max-Mahalanobis Anchors (MMA) to achieve these properties.

We approach the problem from the perspective of angular relationships between anchors, aiming to maximize the minimum angle between any pair of distinct anchors. Mathematically, denoting the angle between anchors μ_i and μ_j as θ_{ij}, we formulate the problem as: $\boldsymbol{\mu}^* = \arg\max_{\boldsymbol{\mu}} \min_{i \ne j} \theta_{ij}$. Intuitively, this criterion aims to maximize the angle between any two centers, which means that the anchors are as distant from each other as possible in the anchor feature space. Such dispersion enhances the model's discrimination capacity by reducing inter-cluster overlap, as demonstrated in (Pang, Du, and Zhu 2018; Pang et al. 2020). However, it is difficult to directly manipulate angles when generating anchors, so we instead manipulate the Mahalanobis distance to generate the desired anchors. We define the Mahalanobis distance between any two anchors μ_i and μ_j as $\Delta_{ij} = \left[(\mu_i - \mu_j)\Sigma^{-1}(\mu_i - \mu_j)\right]^{\frac{1}{2}}$, and the target problem can be equivalently transformed into the following form:

$$\boldsymbol{\mu}^* = \arg\max_{\Delta} \min_{i \ne j} \frac{1}{2}\Delta_{ij}^2. \tag{2}$$

Denoting the minimal distance as $\text{MiD} = \min_{i \ne j} \frac{1}{2}\Delta_{ij}^2$ and $\|\mu_i\|_2^2 = C, \forall i \in [K]$, where C is a positive constant, the following theorem provides a tight upper bound of MiD.

Theorem 1. *Given a set of anchors $\boldsymbol{\mu} = \{\mu_i\}_{i=1}^K$ where $\sum_{i=1}^K \mu_i = \mathbf{0}_K$ and $\|\mu_i\|_2^2 = C$, we can derive an upper bound for* MiD*:*

$$\text{MiD} \le \frac{KC}{K-1}.$$

The equality holds if and only if

$$\mu_i^\top \mu_j = \begin{cases} C & i = j, \\ C/(1-K) & i \ne j, \end{cases} \tag{3}$$

where $1 \le i < j \le K$. See Appendix for detailed proof.

A set of anchors that satisfies Eq. (3) is the optimal anchors $\boldsymbol{\mu}^*$, denoted as Max-Mahalanobis Anchors (MMA) in this paper, indicating that they reach the maximum of the minimal Mahalanobis distance between any two distinct anchors. To achieve this condition, we design the following strategy to obtain anchors that meet the desired criteria:

a) Initialization: Initialize $\mu_1^* = e_1$ and $\mu_i^* = 0_K \ \forall i \geq 2$, where $e_1 = [1, 0, \cdots, 0]^T \in \mathbb{R}^K$ is first unit basis vector and 0_K is a K-dimension zero vector.

b) Recursive generation: Starting from μ_2^*, recursively generate anchors according to Eq. (4):

$$\mu_i^*(j) = \begin{cases} -\frac{\frac{1}{K-1} + \langle \mu_i^*, \mu_j^* \rangle}{\mu_j^*(j)} & j \neq i, \\ \sqrt{1 - \|\mu_i^*\|_2^2} & j = i, \end{cases} \tag{4}$$

where $2 \leq i \leq K$ and $1 \leq j \leq i$.

c) Uniform scaling: Apply a uniform scaling to the anchors by setting $\mu_k^* = \sqrt{C} \cdot \mu_k^*, \forall k \in [K]$.

Upon completing the design of MMA, we demonstrate through Theorems 2 and Theorems 3 that the optimal $\boldsymbol{\mu}^*$ generated by MMA satisfy the aforementioned properties defined in Definition 1-3.

Theorem 2. *Our Max-Mahalanobis Anchors $\boldsymbol{\mu}^*$ satisfies the Diversity property in Definition 1, i.e., the average angle between any two distinct anchors in $\boldsymbol{\mu}^*$ lies between $90°$ and $180°$.*

Proof. Since our MMA $\boldsymbol{\mu}^*$ satisfies Eq. (3), when $C = 1$, the angle θ_{ij} between any μ_i and μ_j is constant, i.e.,

$$\theta_{ij} = \arccos\left(\frac{\mu_i^\top \mu_j}{\|\mu_i\|_2 \|\mu_j\|_2}\right) = \arccos\left(\frac{1}{1-K}\right),$$

where $1 \leq i < j \leq K$ and K is the number of clusters. Therefore, the average angle satisfies

$$\bar{\theta} = \frac{2}{K(K-1)} \sum_{1 \leq i < j \leq K} \theta_{ij} = \arccos(\frac{1}{1-K}).$$

Given that $K \geq 2$ (as there must be at least two clusters), we have $\frac{1}{1-K} \in [-1, 0)$, consequently $\bar{\theta} \in (90°, 180°]$. □

Theorem 3. *Our Max-Mahalanobis Anchors $\boldsymbol{\mu}^*$ possess the Balance property in Definition 2. Particularly, the angles between any two distinct anchors in $\boldsymbol{\mu}^*$ are the same and the variance of them is thus zero.*

Proof. Similar to the proof of Theorem 2, the angle θ_{ij} between any two distinct anchors is constant, i.e., $\theta_{ij} = \arccos(\frac{1}{1-K}), 1 \leq i < j \leq K$. Let $\Theta = \{\theta_{ij} | i \neq j\}$, the variance of the angles between any two distinct anchors satisfies $\text{Var}(\Theta) = 0$, indicating that the MMA possess the *Balance* property with $\varepsilon = 0$. □

To elucidate the *Compactness* of MMA, we provide an intuitive understanding of the shape of MMA in low-dimensional cases. When $K = 2$, the MMA correspond to two vertices of a line segment. For $K = 3$, they form three vertices of an equilateral triangle. In the case of $K = 4$, the MMA correspond to the four vertices of a regular tetrahedron. This geometrical phenomenon demonstrates that the anchors generated by our MMA strategy are confined to $K - 1$ dimensions space, which is more compact compared to the d_i dimensions of fixed anchors in the original data space and the K dimensions of orthogonal anchors. The lower-dimensional manifold on which our MMA are distributed offers advantages in measuring distances for clustering tasks in high-dimensional data space.

A detailed comparison of the properties of fixed, optimized, and the proposed MMA anchors is in the Appendix.

3.3 MMA Guidance for Multi-view Clustering

Having obtained a set of rationally designed anchors $\boldsymbol{\mu}^*$ by MMA, we aim to establish mappings from multiple views to these shared optimal anchors. Given the multi-view dataset $\mathcal{X} = \{\mathbf{X}^{(i)}\}_{i=1}^V$ composed of V views and N instances, where $\mathbf{X}^{(i)} \in \mathbb{R}^{N \times d_i}$ and d_i is the dimension of the samples from i-view. Typically, we have the following objective:

$$\min_{\mathbf{B}, \{\mathbf{P}^{(i)}\}_{i=1}^V, \boldsymbol{\gamma}} \sum_{i=1}^V \gamma_i^2 \|\mathbf{X}^{(i)} - \mathbf{B}\boldsymbol{\mu}^* \mathbf{P}^{(i)}\|_F^2 + \lambda \|\mathbf{B}\|_F^2 \tag{5}$$

$$\text{s.t. } \mathbf{P}^{(i)} \mathbf{P}^{(i)^\top} = \mathbf{I}_K, \mathbf{B} \geq 0, \mathbf{B}\mathbf{1}_K = \mathbf{1}_N, \boldsymbol{\gamma}^\top \mathbf{1}_V = 1.$$

In Eq. (5), $\boldsymbol{\mu}^* \in \mathbb{R}^{K \times K}$ is fixed to be our designed MMA. The cross view $\mathbf{B} \in \mathbb{R}^{N \times K}$ is the new consensus representation of multi-view data. $\mathbf{P}^{(i)} \in \mathbb{R}^{K \times d_i}$ is the i-th view projection between MMA space and original data space.

In the following, we employ the coordinate descent method to solve the optimization problem Eq. (5), optimizing one variable at a time while keeping the others fixed. Specifically, the optimization comprises three steps:

1) **Optimize $\{\mathbf{P}^{(i)}\}_{i=1}^V$ while fixing $\mathbf{B}$ and $\boldsymbol{\gamma}$.** For each view, the optimization goal w.r.t. $\mathbf{P}^{(i)}$ can be simplified to $\max_{\mathbf{P}^{(i)}} \text{Tr}(\mathbf{P}^{(i)^\top} \mathbf{M}_i)$ by expanding the objective and ignoring irrelevant terms, where $\mathbf{M}_i = \boldsymbol{\mu}^{*\top} \mathbf{B}^\top \mathbf{X}^{(i)}$. Assuming the singular value decomposition (SVD) of $\mathbf{M}_i$ is $\mathbf{M}_i = \mathbf{U}_m \Sigma_m \mathbf{V}_m^\top$, the optimal $\mathbf{P}^{(i)}$ is given by $\mathbf{P}^{(i)} = \mathbf{U}_m \mathbf{V}_m^\top$ (Wang et al. 2019).

2) **Optimize $\mathbf{B}$ while fixing $\boldsymbol{\gamma}$ and $\{\mathbf{P}^{(i)}\}_{i=1}^V$.** The optimization problem can be rewritten as the following Quadratic Programming (QP) problem. For each row in $\mathbf{B}$,

$$\min_{\mathbf{b}_j} \frac{1}{2} \mathbf{b}_j \mathbf{Q} \mathbf{b}_j^\top + \mathbf{c}^\top \mathbf{b}_j^\top, \text{ s.t. } \mathbf{b}_j \mathbf{1} = 1, \mathbf{b}_j \geq 0, \tag{6}$$

where $\mathbf{b}_j = \mathbf{B}_{[j,:]} \in \mathbb{R}^{1 \times K}$ refers to the j-th row of $\mathbf{B}$. $\mathbf{Q} = \sum_{i=1}^V \gamma_i^2 \boldsymbol{\mu}^* \boldsymbol{\mu}^{*\top} + \lambda \mathbf{I}_K$ is a symmetric matrix, and $\mathbf{c}^\top = -\sum_{i=1}^V \gamma_i^2 \mathbf{X}_{[j,:]}^{(i)} \mathbf{P}^{(i)^\top} \boldsymbol{\mu}^{*\top}$. Therefore, the optimization problem for $\mathbf{B}$ is transformed into solving QP problems for each row $\mathbf{b}_j$, which can be efficiently solved and parallelized to accelerate the calculation.

3) **Optimize $\boldsymbol{\gamma}$ while fixing $\mathbf{B}$ and $\{\mathbf{P}^{(i)}\}_{i=1}^V$.** Setting $\beta_i = \|\mathbf{X}^{(i)} - \mathbf{B}\boldsymbol{\mu}^* \mathbf{P}^{(i)}\|_F^2$, we can obtain the following problem: $\min_{\boldsymbol{\gamma}} \sum_{i=1}^V \gamma_i^2 \beta_i$, s.t. $\boldsymbol{\gamma}^\top \mathbf{1} = 1, \boldsymbol{\gamma} \geq 0$, where $\boldsymbol{\gamma} = [\gamma_1; \cdots; \gamma_V] \in \mathbb{R}^V$. The optimal $\boldsymbol{\gamma}$ can be obtained by $\gamma_i = \frac{\frac{1}{\beta_i}}{\sum_{i=1}^V \frac{1}{\beta_i}}$ according to the Cauchy-Schwarz inequality.

Algorithm 1: MMA guidance for multi-view clustering

Input: Multi-view data $\{\mathbf{X}^{(i)}\}_{i=1}^{V}$, constant C, clusters K.
Initialize: Initialize $\mathbf{B}$ by concatenating the identity matrix and the zero matrix. Initialize γ_i with the average weight $\frac{1}{V}$.

1: Generate Max-Mahalanobis Anchors $\boldsymbol{\mu}^*$ by Eq. (4).
2: **while** not converged **do**
3: Update $\mathbf{P}^{(i)} = \mathbf{U}_m \mathbf{V}_m^\top$.
4: Update $\mathbf{B}$ by solving problem Eq. (6).
5: Update $\gamma_i = \frac{\frac{1}{\beta_i}}{\sum_{i=1}^{V} \frac{1}{\beta_i}}$.
6: **end while**

Output: Perform k-means on the left singular vector $\mathbf{U}_b$ of $\mathbf{B}$ to obtain the final clustering results.

The optimization process is delineated in Algorithm 1 while the overall algorithm, including the generation of MMA, is detailed in the appendix. To demonstrate the guidance of our MMA on the consensus representation learning, we derive the first-order derivative* of the objective function in Eq. (5) w.r.t. $\mathbf{B}$, which is given by $\nabla \mathcal{J}(\mathbf{B}) = 2\mathbf{B}\mathbf{E} - 2\mathbf{G}{\boldsymbol{\mu}^*}^\top$, where $\mathbf{G} = \sum_{i=1}^{V} \gamma_i^2 \mathbf{X}^{(i)} {\mathbf{P}^{(i)}}^\top$ and $\mathbf{E} = \sum_{i=1}^{V} \gamma_i^2 \boldsymbol{\mu}^* {\boldsymbol{\mu}^*}^\top + \lambda \mathbf{I}_K$. After each gradient update, the new consensus representation can be formulated as:

$$\mathbf{B}_{t+1} = \mathbf{B}_t - \nabla \mathcal{J}(\mathbf{B}) = \mathbf{B}_t(\mathbf{I}_K - 2\mathbf{E}) + 2\mathbf{G}{\boldsymbol{\mu}^*}^\top. \quad (7)$$

Eq. (7) shows that the new representation is actually an interpolation between the previous one and our MMA, i.e. $\boldsymbol{\mu}^*$. Given a suitable hyperparameter λ, the new data representation $\mathbf{B}$ will progressively converge towards our MMA throughout the iteration. Specifically, the whole objective continually adjusts the data representation to better align with the underlying structure expressed by our well-designed MMA. This alignment process facilitates cluster separation and enhances the learned representation's overall discriminative ability.

4 Experiment

This section compares MAGIC with state-of-the-art methods. We first introduce the datasets, compared methods and the experimental setup, followed by the detailed analysis.

4.1 Experimental Setup

We conduct experiments on ten widely-used datasets: BBC, Wikipedia, Reuters, 100Leaves, Cora, Wiki_fea, ALOI-100, VGGFace, YouTubeFace, CIFAR100, denoted as Ds1–Ds10 in following figures for simplicity. Detailed information is presented in the appendix. We compare our approach with nine methods that encompass both fixed-anchor-based MVC methods (LMVSC (Kang et al. 2020b), SFMC (Li et al. 2020)) and optimized-anchor-based methods (FPMVS (Wang et al. 2021), OMSC (Chen et al. 2022b), AIMC (Chen et al. 2022a) and RCAGL (Liu et al. 2024b)). We also included BMVC (Zhang et al. 2018), a efficient algorithm for large-scale MVC, along with state-of-the-art approaches such as AWMVC (Wan et al. 2023) for large-scale MVC and SMSC (Ma et al. 2024) for subspace MVC.

We adopt the officially released codes for fair comparison. For methods requiring k-means, we run 50 times to obtain the best results. Optimal parameters are determined via grid search within established ranges. The constant C was set to 1, simplifying hyperparameter tuning to only balance parameter λ, which is explored within $\{0.01, 1, 10, 100, 1000\}$ based on previous studies We utilized widely used clustering metrics such as Accuracy (ACC), Normalized Mutual Information (NMI), Purity and Fscore, where higher values indicate better performance. All experiments are conducted using MATLAB 2023b on the system equipped with an AMD EPYC 7513 32-Core Processor and 64GB of memory.

4.2 Clustering Performance

We compare our method with nine competing algorithms on ten datasets. The comparison results are presented in Tab. 2, from which the following observations can be drawn.

(1) Our method surpasses competitors on most metrics, achieving the highest ACC and NMI across all datasets. It improves by 18.25%, 7.92%, 6.00%, 11.08%, and 7.22% over the second-best method on the BBC, Reuters, 100Leaves, Cora, and Wiki_fea datasets, respectively, with similar gains across other metrics. This demonstrates the superiority of our approach's clustering performance.

(2) Our method shows robust performance across diverse datasets, from text to image domains, demonstrating adaptability to different multi-view data types. It also excels on datasets with many clusters, achieving the best ACC, NMI, and F-score on ALOI-100, VGGFace, and CIFAR100, highlighting its effectiveness in complex clustering scenarios.

(3) Our MAGIC method consistently outperforms fixed-anchor-based MVC methods (LMVSC and SFMC) and optimized-anchor-based MVC methods (FPMVS, OMSC, AIMC, and RCAGL) across all datasets, demonstrating the effectiveness of our well-designed anchor properties and model validity. Besides, optimized-anchors methods generally outperform fixed-anchor methods due to the orthogonal constraints that promote diversity and balance of anchors.

To illustrate our method's advantages, we visualize the new data representations $\mathbf{B}$ and optimal anchors $\boldsymbol{\mu}^*$ in Fig. 1, comparing them to FPMVS and OMSC on BBC and Wiki_fea datasets. In the left panel of Fig. 1, in terms of BBC dataset, the anchors (red pentagrams) in FPMVS and OMSC collapse, causing the representations (dots) to be incorrectly aggregated. However, our method achieves a more spatially diverse placement of anchors, leading to more discriminative representations, as reflected in the more dispersed distribution of dots. On the Wiki_fea dataset in the right panel of Fig. 1, our approach achieves a more balanced anchor distribution than others, leading to compact intra-cluster and distinct inter-cluster separations. This demonstrates the effectiveness of our anchors in improving clustering structures. The visual evidence aligns with quantitative results, highlighting our method's ability to enhance *Diversity, Balance* and *Compactness*, reducing representation collapse and improving representation learning across multiple views.

*We omit the constraints for the purposes of interpretation.

Dataset	BMVC	LMVSC	SFMC	FPMVS	OMSC	AIMC	AWMVC	SMSC	RCAGL	Proposed
						ACC				
BBC	55.91	40.29	33.58	32.26	35.91	27.15	65.55	37.23	54.75	**83.80**
Wikipedia	19.05	21.79	46.75	32.61	37.95	56.85	23.95	32.32	30.88	**60.90**
Reuters	35.67	39.83	17.25	41.42	45.42	46.58	44.25	47.50	47.58	**55.50**
100Leaves	71.81	55.75	70.88	34.88	36.56	31.75	72.13	64.81	60.56	**78.13**
Cora	32.57	33.20	30.28	55.76	55.54	31.50	39.18	42.25	50.44	**66.84**
Wiki_fea	43.16	18.70	20.03	31.47	36.74	54.29	21.70	41.42	30.81	**61.51**
ALOI-100	62.86	55.32	67.20	32.95	35.02	31.60	69.22	53.20	39.41	**73.77**
VGGFace	10.29	7.48	3.67	9.70	9.71	10.30	14.52	9.41	12.97	**15.61**
YouTubeFace	47.58	78.79	35.61	71.49	78.26	76.02	83.61	OOM	78.68	**86.55**
CIFAR100	7.71	7.27	1.60	7.16	7.49	7.39	10.77	OOM	9.58	**11.82**
						NMI				
BBC	29.10	10.09	1.87	2.97	6.86	2.69	41.33	18.95	30.34	**62.31**
Wikipedia	6.08	6.47	48.71	17.34	25.60	53.92	11.31	19.75	17.36	**54.06**
Reuters	16.24	21.40	1.46	21.10	20.41	24.54	20.14	22.63	26.04	**30.57**
100Leaves	86.22	79.02	86.33	70.22	74.06	71.32	85.48	82.68	84.43	**90.36**
Cora	10.10	6.93	0.54	30.02	29.78	10.05	24.08	20.68	31.23	**45.43**
Wiki_fea	35.84	5.14	14.31	17.15	21.12	51.87	7.83	31.37	15.02	**54.66**
ALOI-100	76.36	72.58	75.73	64.39	68.56	64.93	81.90	69.16	70.67	**83.05**
VGGFace	14.48	9.41	1.59	12.75	13.12	14.25	17.72	11.06	16.55	**19.27**
YouTubeFace	55.84	82.49	48.46	77.40	82.83	83.35	83.66	OOM	80.89	**84.81**
CIFAR100	13.50	13.57	1.79	13.62	14.19	14.26	17.83	OOM	17.57	**17.83**
						Purity				
BBC	55.91	**87.03**	33.87	37.37	40.58	34.60	65.55	39.12	78.10	83.80
Wikipedia	22.37	46.18	51.08	35.79	43.00	60.90	26.70	34.63	35.50	**61.62**
Reuters	39.83	48.50	17.42	45.33	45.83	46.58	46.58	47.50	52.00	**57.25**
100Leaves	74.81	67.94	72.75	36.63	36.94	32.81	75.06	68.06	80.44	**81.00**
Cora	36.48	**95.61**	30.39	55.76	55.54	38.48	46.20	46.79	63.89	66.84
Wiki_fea	47.17	36.36	23.17	33.67	38.97	60.68	25.47	43.86	34.12	**62.81**
ALOI-100	64.95	64.51	68.20	33.61	36.15	32.82	70.84	55.25	**75.22**	75.08
VGGFace	11.83	10.42	3.84	9.97	10.14	10.83	15.83	10.41	**18.81**	16.65
YouTubeFace	55.26	83.30	42.06	76.22	83.03	84.90	83.74	OOM	84.80	**86.57**
CIFAR100	8.51	10.08	1.88	7.34	7.63	7.56	12.09	OOM	**21.15**	12.89
						Fscore				
BBC	42.90	37.61	37.97	27.59	28.75	24.77	51.38	40.88	48.55	**73.64**
Wikipedia	12.42	17.62	32.26	21.12	26.65	49.42	15.04	20.52	19.09	**50.72**
Reuters	26.70	28.87	28.41	30.64	32.86	33.22	30.86	32.51	33.79	**40.35**
100Leaves	62.25	41.54	35.48	22.42	20.82	17.51	62.28	53.57	47.37	**71.23**
Cora	23.41	30.88	30.39	37.35	37.16	21.91	31.70	29.85	38.43	**48.39**
Wiki_fea	35.92	15.82	19.09	21.46	23.77	48.07	14.32	30.97	19.30	**54.84**
ALOI-100	50.04	41.31	12.05	17.99	19.50	13.32	57.73	35.43	24.06	**59.73**
VGGFace	5.34	3.73	4.15	5.75	5.70	5.79	7.50	4.21	6.73	**8.03**
YouTubeFace	42.02	77.38	29.40	69.60	74.63	77.77	**83.28**	OOM	66.49	79.78
CIFAR100	3.47	3.01	1.98	3.40	3.46	3.40	4.49	OOM	4.14	**5.01**

Table 2: The clustering performance comparison across ten datasets. The best results are in bold, while the second-best results are indicated with an underline. "OOM" denotes that the algorithm encountered an out-of-memory error on our device.

4.3 Running Time

The overall time complexity of the proposed MAGIC method is $\mathcal{O}(N)$. Due to space limitations, the detailed analysis process, as well as the complexity reduction achieved compared to optimized-anchor methods, is provided in the appendix. Runtime comparison across all datasets are shown in Fig. 2, with y-axis on a $\log_{10}$ scale. Our method shows competitive efficiency, performing well on smaller datasets like BBC and Wikipedia, outpacing several baselines. Our approach maintains reasonable runtime while some methods fail to complete for larger, complex datasets (e.g., VGGFace, YouTubeFace, CIFAR100). Despite occasional faster runtimes from BMVC and AIMC, our method consistently offers superior performance with acceptable runtime.

4.4 Convergence and Parameter Analysis

The convergence curve in Fig. 3a using Wiki_fea as an example, shows that the objective function value decreases monotonically and then stabilizes, confirming the convergence of

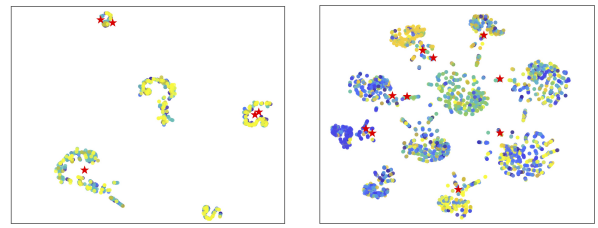

(a) BBC (FPMVS) (b) Wiki_fea (FPMVS)

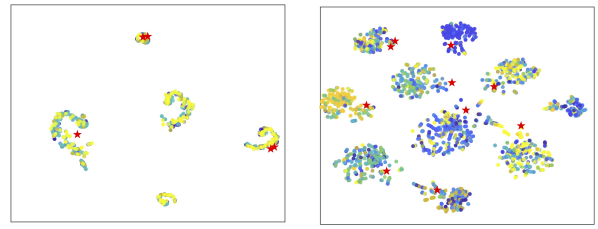

(c) BBC (OMSC) (d) Wiki_fea (OMSC)

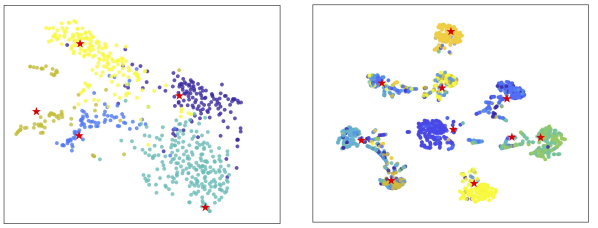

(e) BBC (MAGIC) (f) Wiki_fea (MAGIC)

Figure 1: Comparison of feature and anchor visualizations using t-SNE on BBC and Wiki_fea datasets.

the algorithm. The accuracy curve steadily increases during the iterations, reaching its maximum value when the objective converges, and then remains constant.

The proposed method has one hyperparameter λ, which balances the regularization term. Fig. 3b shows accuracy results across datasets under different λ. Our method performs stable, achieving satisfactory accuracy for λ ranging from 10 to 1000, demonstrating robustness to λ selection. Generally, we recommend $\lambda = 10$ for most datasets.

4.5 Ablation Study

We conduct an ablation study to assess the effectiveness of proposed MMA in anchor-based MVC methods. Orthogonal anchors in SMVSC, OMSC and AIMC are replaced with our proposed MMA, denoted by appending "-MMA". For a fair comparison, the number of anchors is set to K and $\triangle$ indicates the variation relative to the original method. Tab. 3 shows the accuracy improvements with MMA substitution. SMVSC-MMA significantly outperforms SMVSC, with improvements from +10.08% to +47.89%. Similarly, AIMC-MMA consistently surpasses AIMC. OMSC-MMA improves in most cases, notably on YouTubeFace dataset (+4.98%), with a slight decrease on ALOI-100. These results validate our MMA's effectiveness in boosting MVC accuracy, highlighting its potential for further applications. A more detailed comparison between fixed-anchors and optimized-anchors is provided in the appendix.

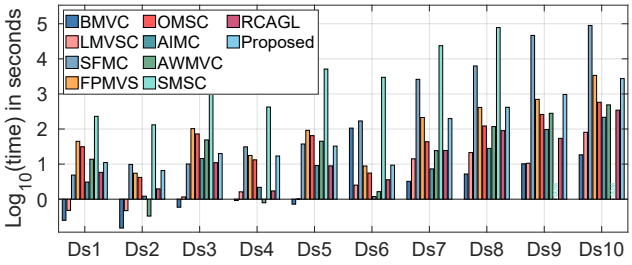

Figure 2: Runtime across ten datasets (Ds1–Ds10).

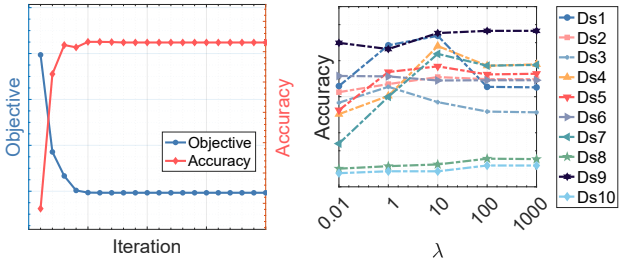

(a) Convergence (b) The impact of λ

Figure 3: Convergence curves and parameter analysis.

Method	BBC	100Leaves	ALOI-100	YouTubeFace
SMVSC	35.91	38.19	34.82	76.47
SMVSC-MMA	83.80	78.13	73.77	86.55
$\triangle$	(+47.89)	(+39.94)	(+38.95)	(+10.08)
OMSC	32.41	34.31	32.91	71.49
OMSC-MMA	35.91	34.94	32.69	76.47
$\triangle$	(+3.50)	(+0.62)	(-0.22)	(+4.98)
AIMC	27.15	31.75	31.60	76.02
AIMC-MMA	28.91	32.56	33.91	76.44
$\triangle$	(+1.75)	(+0.81)	(+2.31)	(+0.42)

Table 3: Ablation study of MMA's impact on accuracy.

5 Conclusion

This paper introduces MAGIC, a novel approach addressing the limitations of existing anchor-based MVC methods. Firstly, we theoretically formalize the properties of *Diversity*, *Balance* and *Compactness* inherent in anchors. Then, we propose a rational strategy MMA, considering inter-anchor Mahalanobis distances to meet the properties with theoretical guarantees. Furthermore, MAGIC iteratively aligns features with well-designed MMA, enhancing representation discriminability and cluster clarity, thereby improving MVC performance. Experiments confirm our MMA's superiority in MVC. Additionally, our approach is applicable to any task requiring anchors. Future work includes a deeper exploration of anchor properties and their integration with multi-view scenarios.

Acknowledgments

This work is supported by National Science and Technology Innovation 2030 Major Project under Grant No. 2022ZD0209103, and National Science Fund for Distinguished Young Scholars of China under Grant 62325604, and National Natural Science Foundation of China (project No. 62476281, 62406329, 62476280), and National Natural Science Foundation of China Joint Found under Grant No. U24A20323, and China Scholarship Council under Grant 202306110002. Yuangang Pan and Ivor Tsang is supported by the A*STAR Centre for Frontier AI Research.

References

Chen, M.-S.; Liu, T.; Wang, C.-D.; Huang, D.; and Lai, J.-H. 2022a. Adaptively-weighted integral space for fast multiview clustering. In *Proceedings of the 30th ACM international conference on multimedia*, 3774–3782.

Chen, M.-S.; Wang, C.-D.; Huang, D.; Lai, J.-H.; and Yu, P. S. 2022b. Efficient orthogonal multi-view subspace clustering. In *Proceedings of the 28th ACM SIGKDD conference on knowledge discovery and data mining*, 127–135.

Gao, H.; Nie, F.; Li, X.; and Huang, H. 2015. Multi-view subspace clustering. In *Proceedings of the IEEE international conference on computer vision*, 4238–4246.

Jin, J.; Wang, S.; Dong, Z.; Liu, X.; and Zhu, E. 2023. Deep incomplete multi-view clustering with cross-view partial sample and prototype alignment. In *Proceedings of the IEEE/CVF conference on computer vision and pattern recognition*, 11600–11609.

Kang, Z.; Zhao, X.; Peng, C.; Zhu, H.; Zhou, J. T.; Peng, X.; Chen, W.; and Xu, Z. 2020a. Partition level multiview subspace clustering. *Neural Networks*, 122: 279–288.

Kang, Z.; Zhou, W.; Zhao, Z.; Shao, J.; Han, M.; and Xu, Z. 2020b. Large-scale multi-view subspace clustering in linear time. In *Proceedings of the AAAI Conference on Artificial Intelligence*, volume 34, 4412–4419.

Li, L.; and He, H. 2020. Bipartite graph based multi-view clustering. *IEEE transactions on knowledge and data engineering*, 34(7): 3111–3125.

Li, L.; Pan, Y.; Liu, J.; Liu, Y.; Liu, X.; Li, K.; Tsang, I. W.; and Li, K. 2024. Bgae: Auto-encoding multi-view bipartite graph clustering. *IEEE Transactions on Knowledge and Data Engineering*.

Li, L.; Zhang, J.; Wang, S.; Liu, X.; Li, K.; and Li, K. 2023a. Multi-view bipartite graph clustering with coupled noisy feature filter. *IEEE Transactions on Knowledge and Data Engineering*, 35(12): 12842–12854.

Li, X.; Sun, Y.; Sun, Q.; Dai, J.; and Ren, Z. 2023b. Distribution Consistency based Fast Anchor Imputation for Incomplete Multi-view Clustering. In *Proceedings of the 31st ACM International Conference on Multimedia*, 368–376.

Li, X.; Zhang, H.; Wang, R.; and Nie, F. 2020. Multiview clustering: A scalable and parameter-free bipartite graph fusion method. *IEEE Transactions on Pattern Analysis and Machine Intelligence*, 44(1): 330–344.

Li, Y.; Nie, F.; Huang, H.; and Huang, J. 2015. Large-scale multi-view spectral clustering via bipartite graph. In *Twenty-Ninth AAAI Conference on Artificial Intelligence*.

Liu, S.; Liang, K.; Dong, Z.; Wang, S.; Yang, X.; Zhou, S.; Zhu, E.; and Liu, X. 2024a. Learn from View Correlation: An Anchor Enhancement Strategy for Multi-view Clustering. In *Proceedings of the IEEE/CVF Conference on Computer Vision and Pattern Recognition*, 26151–26161.

Liu, S.; Liao, Q.; Wang, S.; Liu, X.; and Zhu, E. 2024b. Robust and Consistent Anchor Graph Learning for Multi-View Clustering. *IEEE Transactions on Knowledge and Data Engineering*.

Liu, S.; Wang, S.; Zhang, P.; Xu, K.; Liu, X.; Zhang, C.; and Gao, F. 2022. Efficient one-pass multi-view subspace clustering with consensus anchors. In *Proceedings of the AAAI Conference on Artificial Intelligence*, volume 36, 7576–7584.

Ma, H.; Wang, S.; Zhang, J.; Yu, S.; Liu, S.; Liu, X.; and He, K. 2024. Symmetric Multi-view Subspace Clustering with Automatic Neighbor Discovery. *IEEE Transactions on Circuits and Systems for Video Technology*, 1–1.

Ou, Q.; Wang, S.; Zhang, P.; Zhou, S.; and Zhu, E. 2024. Anchor-based multi-view subspace clustering with hierarchical feature descent. *Information Fusion*, 106: 102225.

Pang, T.; Du, C.; and Zhu, J. 2018. Max-Mahalanobis Linear Discriminant Analysis Networks. In Dy, J.; and Krause, A., eds., *Proceedings of the 35th International Conference on Machine Learning*, volume 80 of *Proceedings of Machine Learning Research*, 4016–4025. PMLR.

Pang, T.; Xu, K.; Dong, Y.; Du, C.; Chen, N.; and Zhu, J. 2020. Rethinking Softmax Cross-Entropy Loss for Adversarial Robustness. In *International Conference on Learning Representations*.

Rappoport, N.; and Shamir, R. 2018. Multi-omic and multi-view clustering algorithms: review and cancer benchmark. *Nucleic acids research*, 46(20): 10546–10562.

Sun, M.; Zhang, P.; Wang, S.; Zhou, S.; Tu, W.; Liu, X.; Zhu, E.; and Wang, C. 2021. Scalable multi-view subspace clustering with unified anchors. In *Proceedings of the 29th ACM International Conference on Multimedia*, 3528–3536.

Wan, X.; Liu, X.; Liu, J.; Wang, S.; Wen, Y.; Liang, W.; Zhu, E.; Liu, Z.; and Zhou, L. 2023. Auto-weighted multi-view clustering for large-scale data. In *Proceedings of the AAAI Conference on Artificial Intelligence*, volume 37, 10078–10086.

Wang, S.; Liu, X.; Liu, S.; Jin, J.; Tu, W.; Zhu, X.; and Zhu, E. 2022. Align then fusion: Generalized large-scale multi-view clustering with anchor matching correspondences. *Advances in Neural Information Processing Systems*, 35: 5882–5895.

Wang, S.; Liu, X.; Zhu, E.; Tang, C.; Liu, J.; Hu, J.; Xia, J.; and Yin, J. 2019. Multi-view Clustering via Late Fusion Alignment Maximization. In *Proceedings of the Twenty-Eighth International Joint Conference on Artificial Intelligence, IJCAI-19*, 3778–3784. International Joint Conferences on Artificial Intelligence Organization.

Wang, S.; Liu, X.; Zhu, X.; Zhang, P.; Zhang, Y.; Gao, F.; and Zhu, E. 2021. Fast parameter-free multi-view subspace clustering with consensus anchor guidance. *IEEE Transactions on Image Processing*, 31: 556–568.

Wen, J.; Liu, C.; Xu, G.; Wu, Z.; Huang, C.; Fei, L.; and Xu, Y. 2023. Highly confident local structure based consensus graph learning for incomplete multi-view clustering. In *Proceedings of the IEEE/CVF Conference on Computer Vision and Pattern Recognition*, 15712–15721.

Xia, W.; Gao, Q.; Wang, Q.; Gao, X.; Ding, C.; and Tao, D. 2022. Tensorized bipartite graph learning for multi-view clustering. *IEEE Transactions on Pattern Analysis and Machine Intelligence*, 45(4): 5187–5202.

Yang, B.; Zhang, X.; Li, Z.; Nie, F.; and Wang, F. 2022. Efficient multi-view K-means clustering with multiple anchor graphs. *IEEE Transactions on Knowledge and Data Engineering*, 35(7): 6887–6900.

Yang, B.; Zhang, X.; Nie, F.; Wang, F.; Yu, W.; and Wang, R. 2020. Fast multi-view clustering via nonnegative and orthogonal factorization. *IEEE Transactions on Image Processing*, 30: 2575–2586.

Yang, X.; Jiaqi, J.; Wang, S.; Liang, K.; Liu, Y.; Wen, Y.; Liu, S.; Zhou, S.; Liu, X.; and Zhu, E. 2023. Dealmvc: Dual contrastive calibration for multi-view clustering. In *Proceedings of the 31st ACM International Conference on Multimedia*, 337–346.

Yu, S.; Liu, S.; Wang, S.; Tang, C.; Luo, Z.; Liu, X.; and Zhu, E. 2023. Sparse low-rank multi-view subspace clustering with consensus anchors and unified bipartite graph. *IEEE Transactions on Neural Networks and Learning Systems*.

Yu, S.; Wang, S.; Zhang, P.; Wang, M.; Wang, Z.; Liu, Z.; Fang, L.; Zhu, E.; and Liu, X. 2024. Dvsai: Diverse view-shared anchors based incomplete multi-view clustering. In *Proceedings of the AAAI Conference on Artificial Intelligence*, volume 38, 16568–16577.

Zhang, C.; Wang, S.; Liu, J.; Zhou, S.; Zhang, P.; Liu, X.; Zhu, E.; and Zhang, C. 2021. Multi-view clustering via deep matrix factorization and partition alignment. In *Proceedings of the 29th ACM International Conference on Multimedia*, 4156–4164.

Zhang, P.; Wang, S.; Li, L.; Zhang, C.; Liu, X.; Zhu, E.; Liu, Z.; Zhou, L.; and Luo, L. 2023. Let the data choose: Flexible and diverse anchor graph fusion for scalable multi-view clustering. In *Proceedings of the AAAI Conference on Artificial Intelligence*, volume 37, 11262–11269.

Zhang, T.; Liu, X.; Zhu, E.; Zhou, S.; and Dong, Z. 2022. Efficient anchor learning-based multi-view clustering–a late fusion method. In *Proceedings of the 30th ACM International Conference on Multimedia*, 3685–3693.

Zhang, Z.; Liu, L.; Shen, F.; Shen, H. T.; and Shao, L. 2018. Binary multi-view clustering. *IEEE transactions on pattern analysis and machine intelligence*, 41(7): 1774–1782.